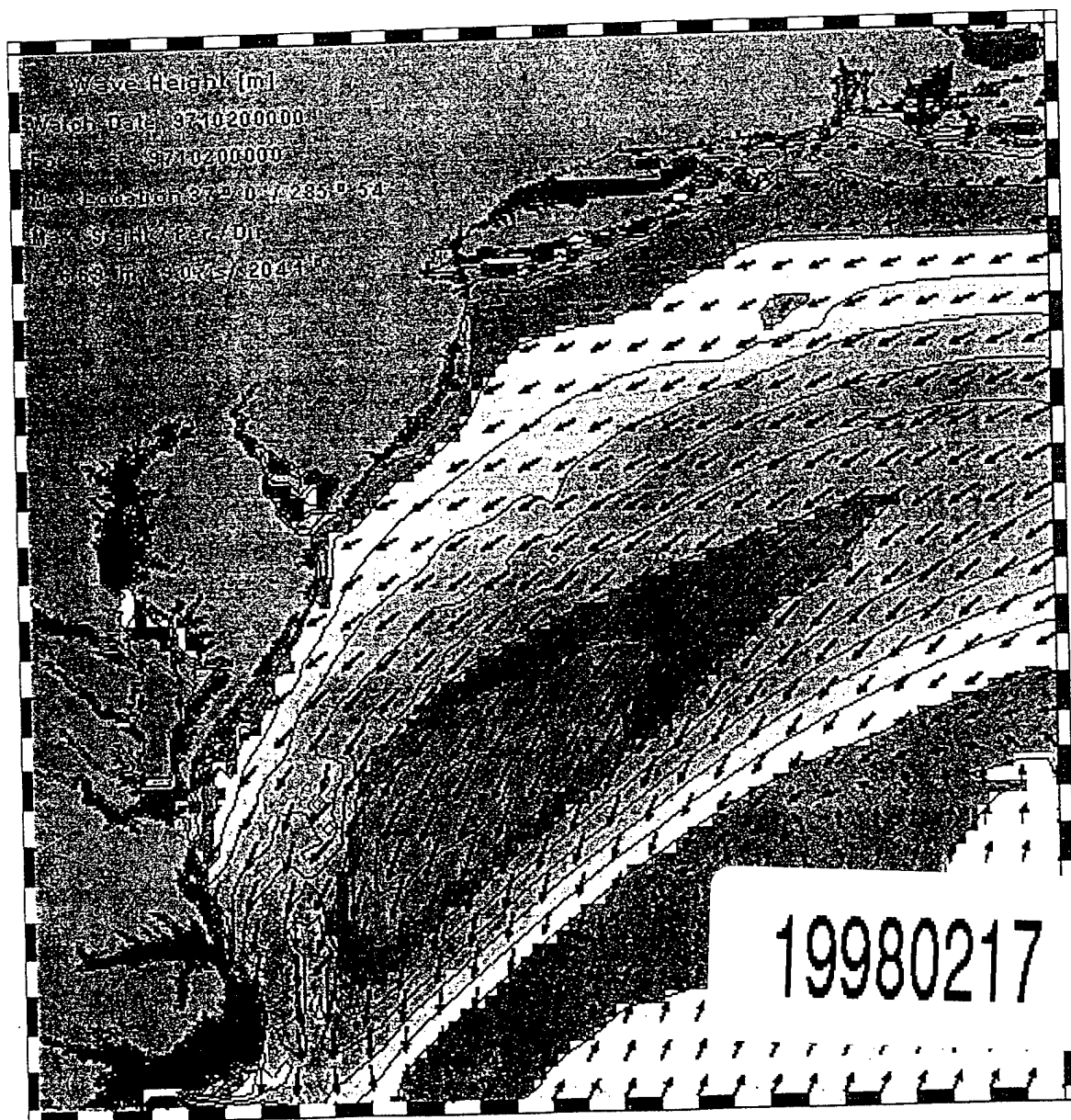


# 5<sup>TH</sup> INTERNATIONAL WORKSHOP ON WAVE HINDCASTING AND FORECASTING

JANUARY 26-30, 1998

MELBOURNE, FL.



USAE WATERWAYS  
EXPERIMENT STATION

FLEET NUMERICAL  
METEOROLOGY AND  
OCEANOGRAPHY CENTER

FLORIDA INSTITUTE OF  
TECHNOLOGY

ATMOSPHERIC  
ENVIRONMENT SERVICE  
CANADA

# REPORT DOCUMENTATION PAGE

Form Approved  
OBM No. 0704-0188

Public reporting burden for this collection of information is estimated to average 1 hour per response, including the time for reviewing instructions, searching existing data sources, gathering and maintaining the data needed, and completing and reviewing the collection of information. Send comments regarding this burden or any other aspect of this collection of information, including suggestions for reducing this burden, to Washington Headquarters Services, Directorate for Information Operations and Reports, 1215 Jefferson Davis Highway, Suite 1204, Arlington, VA 22202-4302, and to the Office of Management and Budget, Paperwork Reduction Project (0704-0188), Washington, DC 20503.

1. AGENCY USE ONLY (Leave blank)		2. REPORT DATE January 1998		3. REPORT TYPE AND DATES COVERED Proceedings	
4. TITLE AND SUBTITLE Use of Phase-Resolving Numerical Wave Models in Coastal Areas				5. FUNDING NUMBERS	
				Job Order No. 73551908 Program Element No. 062435N Project No. Task No. R035E35 Accession No. DN154016	
6. AUTHOR(S) James M. Kaihatu, <sup>1</sup> W. Erick Rogers, Y. Larry Hsu, and <sup>2</sup> William C. O'Reilly					
7. PERFORMING ORGANIZATION NAME(S) AND ADDRESS(ES) Naval Research Laboratory Oceanography Division Stennis Space Center, MS 39529-5004				8. PERFORMING ORGANIZATION REPORT NUMBER NRL/PP/7322--97-0042	
9. SPONSORING/MONITORING AGENCY NAME(S) AND ADDRESS(ES) Office of Naval Research 800 North Quincy Street Arlington, VA 22217-5000				10. SPONSORING/MONITORING AGENCY REPORT NUMBER	
11. SUPPLEMENTARY NOTES Proceedings of 5th International Workshop on Wave Hindcasting and Forecasting, January 26-30, 1998, Melbourne, FL <sup>1</sup> Planning Systems, Inc., MSAAP Building 9121, Stennis Space Center, MS 39529-5004 <sup>2</sup> Department of Oceanography, Naval Postgraduate School, Monterey, CA 93943					
12a. DISTRIBUTION/AVAILABILITY STATEMENT  Approved for public release; distribution unlimited.				12b. DISTRIBUTION CODE	
13. ABSTRACT (Maximum 200 words)  The choice of a particular wave model for use in nearshore wave climate forecasting or hindcasting is usually contingent upon the site to be considered and the processes to be modeled. Phase-averaged spectral models such as SWAN, WAM or STWAVE are source-based energy models which treat the wave field as a stochastic phenomenon. This particular formulation allows for the consideration of wind-wave generation, among other source terms. These models (particularly STWAVE and SWAN) are able to simulate irregular wave propagation over coastal areas relatively efficiently; however, the propagation terms in these models are derived from ray theory and do not handle bathymetrically-induced diffraction, which may be important in coastal areas. (It should be noted that STWAVE does not contain some accounting for diffraction as a diffusion of wave energy in the source terms). Phase-resolving models such as REF/DIF1, REF/DIF-S and RCPWAVE by contrast, treat the wave field deterministically, tracing the free surface evolution over the domain. The irregular nature of the wave field can be accounted for by running several wave frequencies/directions through the model and calculating the statistics from the model results. This is often done by discretizing an input spectrum into frequency and direction bins, calculating the waveheight in each bin and then running them through the model. This formulation is most useful in the case of complex bathymetry and predominantly swell-like conditions. Models in this latter class cannot account for wind-wave generation.					
14. SUBJECT TERMS numerical modeling, waves, forecasting, hindcasting, phase-averaged spectral modeling, SWAN, WAM, STWAVE, REF/DIF1, RCPWAVE, REF/DIF-S, bathymetry, parabolic modeling, and frequency discretization				15. NUMBER OF PAGES 16	
				16. PRICE CODE	
17. SECURITY CLASSIFICATION OF REPORT Unclassified	18. SECURITY CLASSIFICATION OF THIS PAGE Unclassified	19. SECURITY CLASSIFICATION OF ABSTRACT Unclassified	20. LIMITATION OF ABSTRACT SAR		

# USE OF PHASE-RESOLVING NUMERICAL WAVE MODELS IN COASTAL AREAS

James M. Kaihatu<sup>1</sup>, W. Erick Rogers<sup>2</sup>, Y. Larry Hsu<sup>1</sup>, and William C. O'Reilly<sup>3</sup>

<sup>1</sup>Oceanography Division, Code 7322  
Naval Research Laboratory  
Stennis Space Center, MS 39529-5004

<sup>2</sup>Planning Systems, Inc.  
MSAAP Building 9121  
Stennis Space Center, MS 39529-5004

<sup>3</sup>Department of Oceanography  
Naval Postgraduate School  
Monterey, CA 93943

## 1. INTRODUCTION

The choice of a particular wave model for use in nearshore wave climate forecasting or hindcasting is usually contingent upon the site to be considered and the processes to be modeled. Phase-averaged spectral models such as SWAN (Booij et al. 1996), WAM (Komen et al. 1994) or STWAVE (Resio 1988) are source-based energy models which treat the wave field as a stochastic phenomenon. This particular formulation allows for the consideration of wind-wave generation, among other source terms. These models (particularly STWAVE and SWAN) are able to simulate irregular wave propagation over coastal areas relatively efficiently; however, the propagation terms in these models are derived from ray theory and do not handle bathymetrically-induced diffraction, which may be important in coastal areas. (It should be noted that STWAVE does contain some accounting for diffraction as a diffusion of wave energy in the source terms). Phase-resolving models such as REF/DIF1 (Kirby and Dalrymple 1994), REF/DIF-S (Kirby and Ozkan 1994) and RCPWAVE (Ebersole et al. 1986), by contrast, treat the wave field deterministically, tracing the free surface evolution over the domain. The irregular nature of the wave field can be accounted for by running several wave frequencies/directions through the model and calculating the statistics from the model results. This is often done by discretizing an input spectrum into frequency and direction bins, calculating the waveheight in each bin and then running them through the model. This formulation is most useful in the case of complex bathymetry and predominantly swell-like conditions. Models in this latter class cannot account for wind-wave generation.

For performing wave hindcasting or forecasting, however, it may be reasonable to use a "telescoping"

approach. In this scenario, a phase-averaged model (usually WAM) is used to transport wave energy from deep water to the edge of the coastal zone, at which point this energy is then input into a coastal wave model to propagate this energy over the interior domain. The nearshore model would be either a coastal phase-averaged model or a phase-resolving model.

In this study we investigate the use of the phase-resolving wave model REF/DIF1 as a forecasting/hindcasting tool. We will look at both narrow shelf (West Coast) and broad shelf (East Coast) problems; each of these areas has unique bathymetric characteristics and thus requires different approaches. For the narrow-shelf problem, we will outline the use of REF/DIF1 in a forecast mode for a stretch of the Southern California coast. We then investigate the sensitivity of the model results to discretization of the spectrum in both frequency and direction, to confirm that our original discretization for the forecast system was sufficient. We then look at the broad shelf problem and note the frequency and directional discretization effects in this situation.

## 2. BACKGROUND

The difficulty in using phase-resolving wave models to simulate irregular wave evolution is that each monochromatic component exhibits a strong and unique variability over most nearshore bathymetry. In times when computational power was at a premium, the usual method for modeling irregular waves was to use a pseudo-monochromatic approach. This was done by representing the wave spectrum in terms of significant wave height  $H_{1/3}$ , peak period  $T_p$ , and peak direction, and running the wave model with these parameters. Unfortunately the resulting wave field is

still highly variable, and thus the use of these results to calculate such quantities as sediment transport can lead to unrealistic results. This difficulty can be surmounted by running many wave components (representative of a wave spectrum) and then calculate the associated wave statistical parameters; this usually leads to a smoother, more realistic waveheight field. This can be done in either a component-by-component fashion (REF/DIF1 and RCPWAVE) or by running all components simultaneously (REF/DIF-S).

It is not clear, however, how the spectrum should be discretized in order to simulate irregular wave evolution. The frequency and direction bands of the input spectra are usually determined by the measuring instrument and the associated processing software. Nonetheless, the adequacy of representing each frequency-direction band with a single monochromatic component at the center frequency and direction remains an open question. In this study we will investigate the effect of subdividing these prespecified frequency-direction bands into finer bins, and then averaging the waveheights from each individual bin across all bands in order to obtain an averaged result. This average would then represent the band. To this end, O'Reilly and Guza (1993) investigated the effect of spectral discretization on the smoothness of the waveheight field in the Southern California Bight. They initialized their parabolic refraction-diffraction model with spectra recorded at the Harvest Platform (located offshore of Point Conception), and simulated the wave evolution over a domain 300km by 300km. A phase-resolving model was necessary for this application because the wave evolution process needed to account for several large offshore islands in the Bight. O'Reilly and Guza (1993) determined that a significant level of variation in nearshore waveheight (leeward of the islands) existed for a small amount of variation in offshore wave angle (seaward of the islands). Using a nominal spectral discretization of  $5^\circ$  in direction and  $0.01\text{Hz}$  in frequency, they found that there was a substantial difference between waveheights on the coast calculated using one representative frequency and direction for this band, and those calculated by subdividing this bandwidth into finer bins and then averaging the resulting waveheight fields over the band. It can be supposed that the great variability is due to the presence of the islands; small differences in the wave frequency or direction may lead to large differences in the refraction/diffraction pattern around these features, thus clarifying the need for a relatively fine discretization. It is not clear, however, that this is required for an open coast. (We note that different frequency and directional distributions would require different spectral discretizations by virtue of their shape; we do not address this issue in this study.)

### 3. THE NUMERICAL MODELS

The primary model under consideration in this study is REF/DIF1 (Kirby and Dalrymple 1994). This model is monochromatic, and looping of the code to run through desired frequencies and directions is required. The model is a phase-resolving, frequency-domain parabolic approximation of the mild-slope equation for water wave propagation (Berkhoff 1972). The parabolic approximation (Radder 1979) reduces the elliptic mild-slope equation to a parabolic form, thereby allowing the solution to march forward as an initial value problem. Solution of this approximate equation is relatively efficient in memory, since values along only two longshore grid rows need be retained for any one forward step. However, the parabolic approximation assumes that the wave is propagating primarily along the cross-shore ( $x$ ) direction of the domain, and thus significant errors are possible if the wave approaches the grid at angles over about  $20^\circ$  to the  $x$  direction. Additionally, the approximation disallows back reflection of waves, and thus only forward scattered or propagating waves may be represented.

The formulation in REF/DIF1 utilizes the wide-angle approximation of Kirby (1986). This approximation yields additional terms that serve to reduce the angular error between the parabolic approximation and the full elliptic solution without adding any discernible computational difficulty. Waves approaching the domain at angles up to  $45^\circ$  from the  $x$  direction can be modeled without significant error. However, for this study we rotated the grid to several orientations in order to keep the angle of incidence small.

The model REF/DIF1 utilizes the decay model of Dally et al. (1985). This formulation is problematic for irregular waves because each individual wave in the wavetrain has its own decay characteristic and incipient breaking condition. We will detail how this is handled for the West Coast case in the next section.

The model used to generate forcing conditions for the forecast is WAM (Komen et al. 1994). This phase-averaged model is used operationally by oceanographic centers worldwide for wave climate forecasting. It is based on a description of wave evolution as a random phase process. The model contains source/sink terms that account for wave propagation, whitecapping, wind-wave generation, nonlinear interaction, and bottom friction. The wind forcing for the WAM model is provided by the Navy Operational Regional Atmospheric Prediction System (NORAPS), and the 10m elevation winds are used.

#### 4. WEST COAST - NARROW SHELF CASE

We first investigated the use of REF/DIF1 in a forecast mode in modeling a section of the Southern California Bight near Oceanside and Camp Pendleton. We outlined an area near Oceanside, about  $0.5^\circ$  on each side, to run the model; the domain is shown in Figure 1. The narrow width of the shelf is apparent. For bathymetry we used the 3 second by 3 second grid discussed in O'Reilly and Guza (1993) and derived from the National Ocean Survey (NOS) database; this bathymetry was interpolated onto a grid with  $\Delta x = \Delta y = 100m$ . The seaward-most point in the grid corresponded to a location where wave spectra from the WAM model were available. This point was chosen because it appeared to not be affected by the offshore islands. The WAM model is presently being run operationally by the Naval Oceanographic Office (NAVO) at Stennis Space Center, MS, and 48 hour forecasts are run twice daily for selected regional locations, with predicted spectra made available at several points in the Bight. These regional WAM simulations are forced by global WAM results, also run by NAVO. Details on the operational implementation of WAM can be found in Wittmann and Farrar (1997). Furthermore, a Datawell directional buoy was installed near the local shelf break offshore of Oceanside Harbor ( $33.1789^\circ$  latitude,  $117.2531^\circ$  longitude).

As mentioned above, REF/DIF1 contains a wide-angle

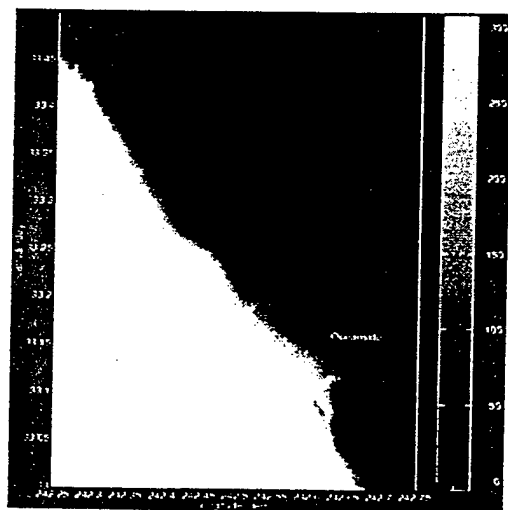


Figure 1: Domain of Study - Southern California Bight. Depths Are In Meters.

correction that allows for fairly large incident angles without a corresponding increase in error. However, we

were able to orient the grid so that we could keep the incident angles reasonably small for all directions except for waves approaching from the northwest, where the incident angles were at most  $45^\circ$  to the x-axis. We had originally intended to orient the grid such that the waves approaching from this direction would have a small incidence angle; however, the close proximity of the coast along the lateral boundary of the grid caused significant noise in the transformation coefficients. Additionally, waves approaching from this direction during this time of year do not make up a significant part of the overall wave climate. Thus, we used the east-west oriented grid to model waves approaching from this sector. The grid orientations used are shown in Figure 2. The west-east and south-north grids had resolutions of  $\Delta x = \Delta y = 100m$ , while the

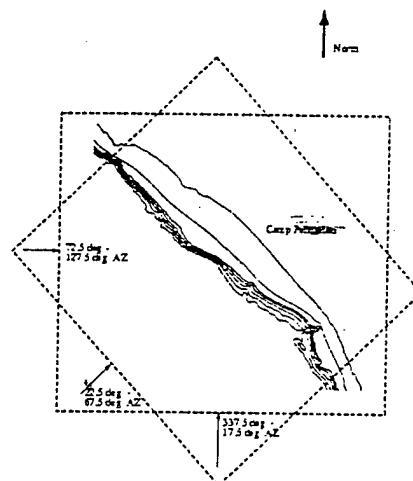


Figure 2: Grid Orientations for Parabolic Model. Grid Overlap Not to Scale.

southeast-northwest grid had resolutions of  $\Delta x = \Delta y = 70.71m$ ; this was done so that the points from the three grids overlapped. During the time of the forecast, when the WAM spectra were discretized and component wave heights through the domain calculated and summed, the results from all three grids were mapped onto the east-west oriented grid.

In anticipation of long computational times we used the "transformation coefficient" approach of O'Reilly and Guza (1993). First, a range of frequencies and directions was chosen, and subdivided into frequency-direction bins. Each bin was then initialized with a unit wave height and run in REF/DIF1, generating fields of transformation coefficients to be stored. A sample

transformation coefficient field is shown in Figure 3. During the forecast time, WAM spectra at the offshore point would then be discretized into the same bands used to run the REF/DIF1 model. Waveheights would be calculated in each band, and this waveheight multiplied by the transformation coefficient field associated with this band. The individual component fields would then be summed to yield significant wave heights and peak direction. We handled the problem of irregular wave breaking by setting all significant waveheights in water less than 2m depth to zero. We also tried to eliminate any anomalously high significant waveheights in the region by restricting their maximum values to be 0.78 of the water depth, corresponding to a pseudo-monochromatic approach.

Based on a sample WAM run from the last week of May 1997, a frequency range of 0.04-0.13Hz and a directional range from 337.5°-127.5° azimuth (where 0° refers to a wave moving from south to north) were used. This frequency range was denoted the "swell range" and thus required the model runs for simulation of wave transformation. In the interests of time we utilized Snell's Law for the frequency range beyond 0.13 Hz, on the supposition that wave energy in this range would not be substantial. The frequency and direction ranges were subdivided into 0.01 Hz and 5° intervals. (For reference, the WAM forecasts from NAVO are discretized at 15° directional intervals,

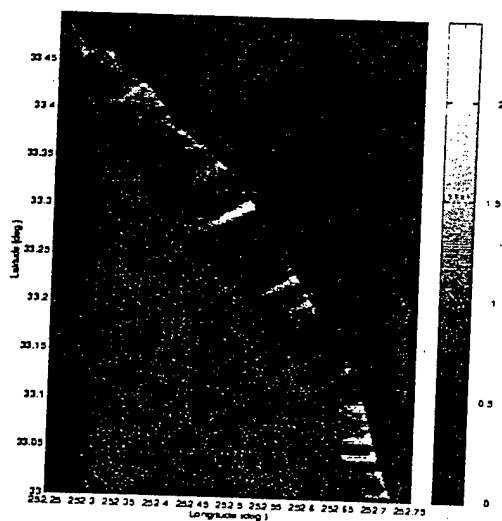


Figure 3: Transformation Coefficient Field for 25s Wave Propagating at 112.5° AZ.

while the frequency intervals increase logarithmically with increasing frequency.) We then ran each bin in the spectrum through the model, and stored the resulting

transformation coefficient fields. Once the WAM spectra were obtained, we ran this spectrum over the transformation coefficient fields, calculated and plotted significant wave height fields and peak direction, and put the plot on a Web page for user access; example are shown in Figures 4 and 5. Some difficulties were encountered with the WAM forecast spectra for this time frame, precluding direct comparison of results with the Datawell buoy. Investigations into the causes of these problems are continuing as of the time of this writing.

However, it is still important to investigate whether the chosen frequency-directional bins were sufficiently fine to bring about smooth wave fields. We noted that O'Reilly and Guza (1993) found that the wavefield resulting from a wave condition at the center of a 5° bin was substantially different from an averaged bin of equal width if the offshore islands were included in the domain. Additionally, we wished to incorporate the spectra from the Datawell buoy into the model. Thus we repositioned the domain somewhat so that the offshore boundary of a grid oriented southwest-northeast was located near both the buoy and the closest WAM output location. We employed the same three-grid system as before. The rotated (southwest-northeast oriented) grid had corners at 33.0227° latitude, 242.6826° longitude; 33.2773° latitude, 242.3774° longitude; 33.5319° latitude, 242.6826° longitude; and 33.2773° latitude, 242.9878° longitude. The north-south and east-west grids were defined to envelop the rotated grid completely. Then the rotated grid was truncated to eliminate the large number of land points. For the ensuing sensitivity tests we used both the rotated grid (x-direction close to shore normal) and the east-west oriented grid.

The rotated grid is tested first. We first tested the sensitivity of the model results with small variations in frequency. This was done for waves with frequencies of 0.05 Hz and 0.10Hz. We defined a frequency bandwidth of 0.01Hz, as was done for the forecast, and first ran a single wave component with unit wave height at the central frequency over the domain. We then ran waves with frequencies of  $\pm 0.001$  Hz from the central frequency over the domain and averaged these bands together to create an averaged bin. Figure 6 shows the results for a 0.05 Hz centered frequency. The top figure shows the results for a single wave component of unit wave height at 0.05 Hz. The middle figure shows the result of an averaged bin in which three frequencies of 0.045 Hz, 0.05 Hz and 0.055 Hz were averaged. The lower figure shows a result of an averaged bin consisting of all 11 frequencies between 0.045-0.055 Hz. There appears to be no substantial

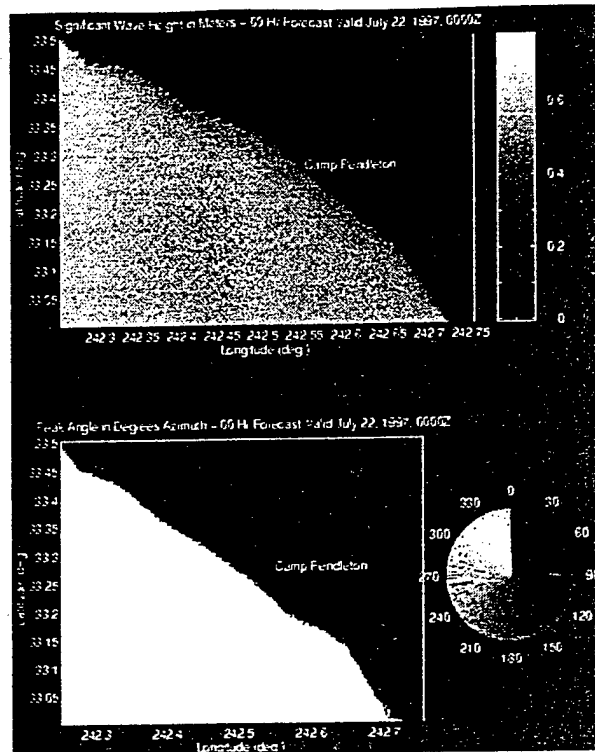


Figure 4: 00Z Hr. Forecast for July 22, 1997

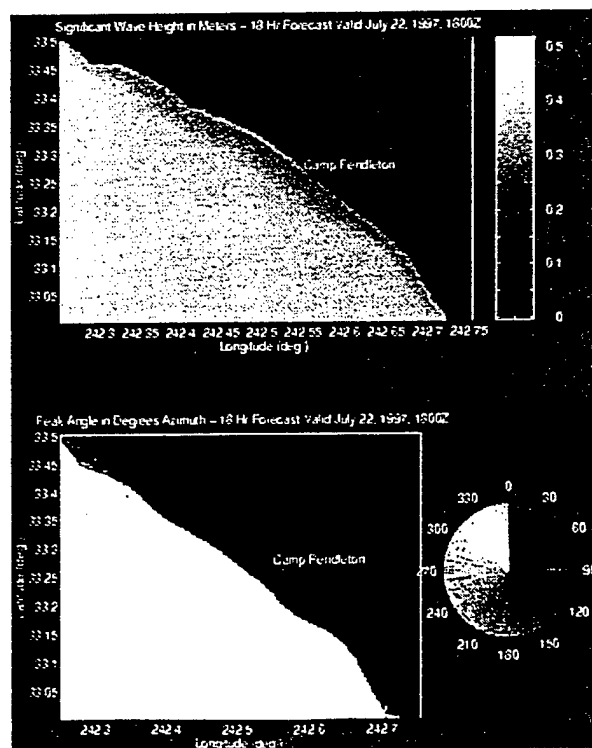


Figure 5: 18Z Hr. Forecast for July 22, 1997

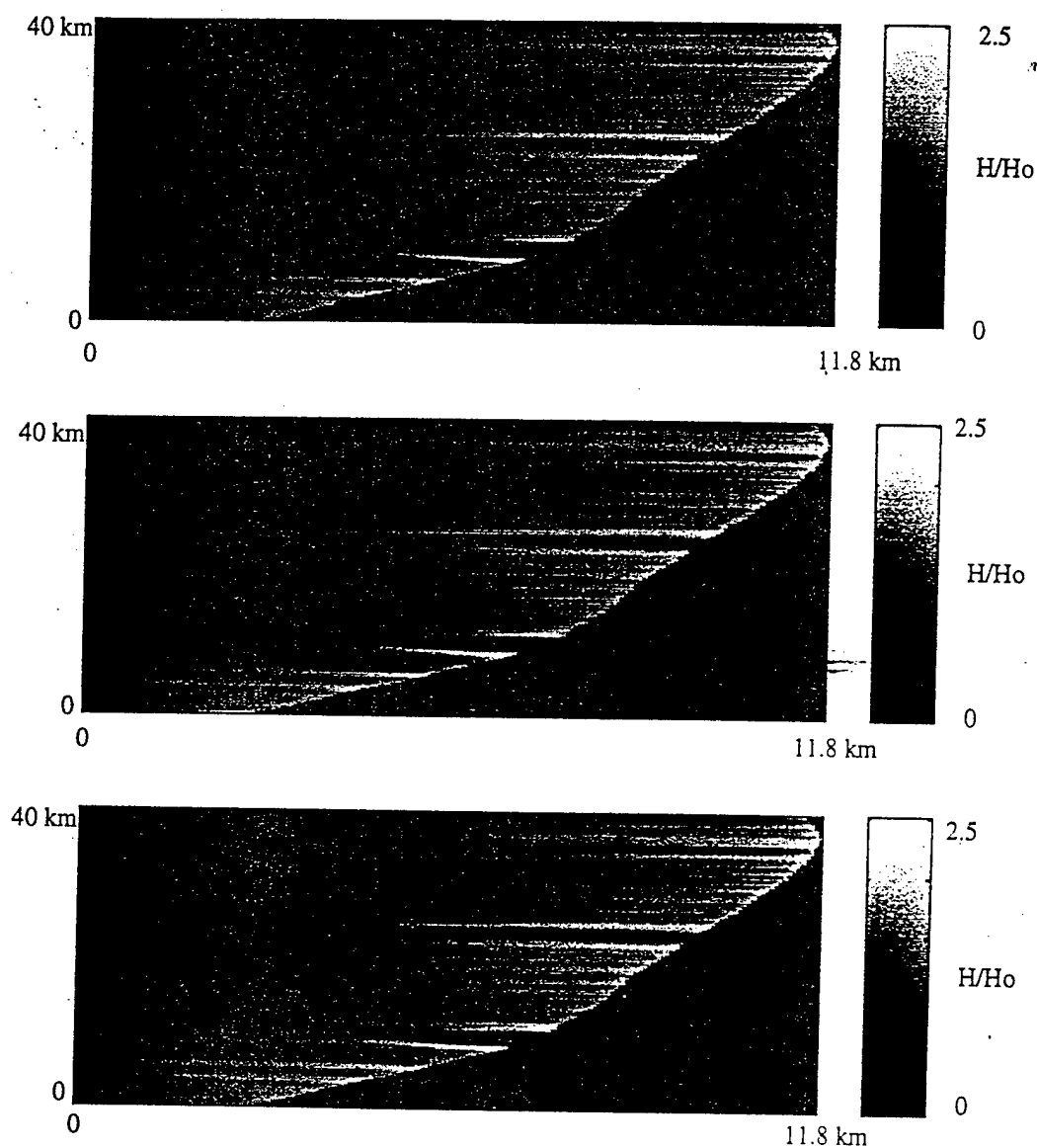


Figure 6: Comparison of Frequency Discretization Methods, Narrow Shelf Case, Rotated Grid,  $T=25s$ , Mean Direction  $45^\circ$  Azimuth. Top:  $H/H_o$  Field for Single Wave Component at Center Frequency and Direction. Middle:  $H/H_o$  Field from Average of Three Components Within Band. Bottom:  $H/H_o$  Field from Average of Eleven Components Within Band. Note: Scale of Abscissa Distorted Relative To Ordinate.



difference between the three plots. Tests were also performed for a wave condition with a centered frequency of 0.10 Hz, where frequencies of 0.095-0.105 Hz were modeled. The results showed similar insensitivity to discretization finer than 0.01 Hz. This shows that the 0.01 Hz bins used for the forecast seem to be sufficiently fine for waves approaching from the southwest.

The sensitivity of the results with respect to incident wave direction was also studied on the rotated grid. We used the same directional bandwidth as the forecast (5°) and used a centered angle of 45° azimuth. We define nine directional bins, each of 0.625° bandwidth, from 42.5° to 47.5° azimuth. We then tested the sensitivity of the model by running waves of 0.05 Hz frequency with unit offshore wave height at these directions, and then averaging the results of several bands together. This test was repeated for the 0.10 Hz wave. As with the wave frequency sensitivity, there was little difference between the results for different discretizations for either frequency, confirming that the 5° directional bins used in the forecasting system were also sufficiently fine for waves approaching from the southwest.

Additionally, the tests were repeated for the east-west oriented grid for a wave approaching at 110° azimuth. This was thought to be a more severe case of wave transformation. Waves moving in this direction would likely undergo a high rate of turning in order to refract around and approach the shoreline. Thus it seems reasonable to believe that there would be appreciable differences in refraction/diffraction patterns between waves of closely-spaced frequencies moving in a narrow band of directions. We performed these tests in the same manner as was done on the rotated grid, and found that very little difference existed between the wavefields calculated either at the centered frequency and direction or in averaged frequency and direction bands. Thus it seems reasonable to conclude that waves approaching from the west to northwest were well represented by the spectral discretizations we chose for the forecast system. (We note here that in the above tests, similarity between wavefields resulting from various discretizations was confirmed by comparison of transects cut through the wavefields. These are not shown, since the waveheights virtually overlaid each other.)

The fact that the model results exhibit little sensitivity to the spectral discretization into bins finer than those used for the forecasting system indicates that the sensitivity to discretization bandwidth seen by O'Reilly and Guza (1993) in the same region is due primarily to the presence of the offshore islands in their domain. In

this case, the offshore boundary condition for the modeling was located well leeward (and out of the shadow zone) of the islands.

Having confirmed the adequacy of the frequency and directional resolution used for the forecast, we then use model on the repositioned grid to simulate the propagation of the wavefield recorded at the buoy location into the domain. At the time of this writing the results for all grids were still undergoing analysis. Thus we show several realizations using only the rotated grid and only calculating the portion of energy in the buoy spectra in which the waves are approaching the coast between 27.5° and 72.5° azimuth, and have frequencies between 0.04 Hz and 0.13 Hz. It is noted here that this was not usually the sector containing the greatest portion of wave energy. Figures 7 and 8 show the results for several realizations of buoy spectra.

It should be noted that the implications of these results on general modeling practice are limited. The sampling of the bathymetry plays a large role. As noted above, the bathymetry used in this study was taken from the NOS database, and not taken specifically for this study. The resolution at which the raw bathymetric soundings were taken varies widely. Interpolation onto a regular latitude by longitude grid can smooth out local features, which are further smoothed by interpolation onto a 100 m by 100 m grid.

We mention here that no attempt to find the "ideal" spectral discretization was made with regard to the narrow shelf case. Our primary intent was to confirm the adequacy of our chosen spectral discretizations for the forecasting system. This is probably sufficient, in light of the relative smoothness of the bathymetry. In the next study, wave propagation over more complex, broad-shelf bathymetry will be examined.

## 5. EAST COAST - BROAD SHELF CASE

The model REF/DIF1 was also used in a forecast mode near Camp Lejeune, NC. Rather than relying solely on the National Ocean Survey database for bathymetry for this area, NRL surveys and a bathymetry database from NAVO were also used and blended in to the NOS bathymetry to better resolve the small scale features in the nearshore area. This is shown in Figure 9. The resolution used here was  $\Delta x = \Delta y = 92.5m$ . The incorporation of WAM spectra from NAVO for use in a wave modeling system is detailed in Allard et al. (1998, this conference). Here we will discuss the impact of the spectral discretization on the model results.

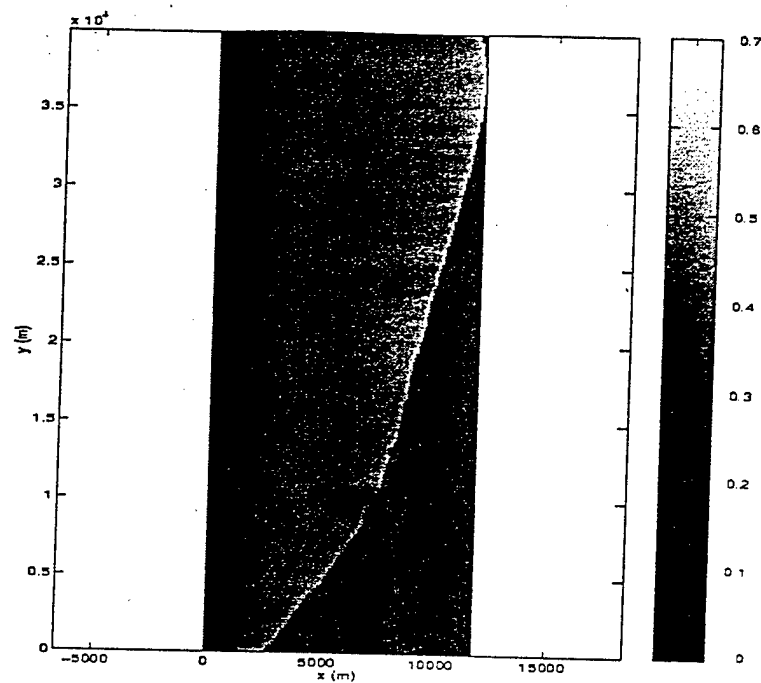


Figure 7: Partial Wave Height Field for July 30, 1997, 1036PST. Model Forced with Portion of Buoy Spectrum ( $27.5^\circ$ - $72.5^\circ$  AZ and 0.04-0.13Hz). Heights are in Meters.

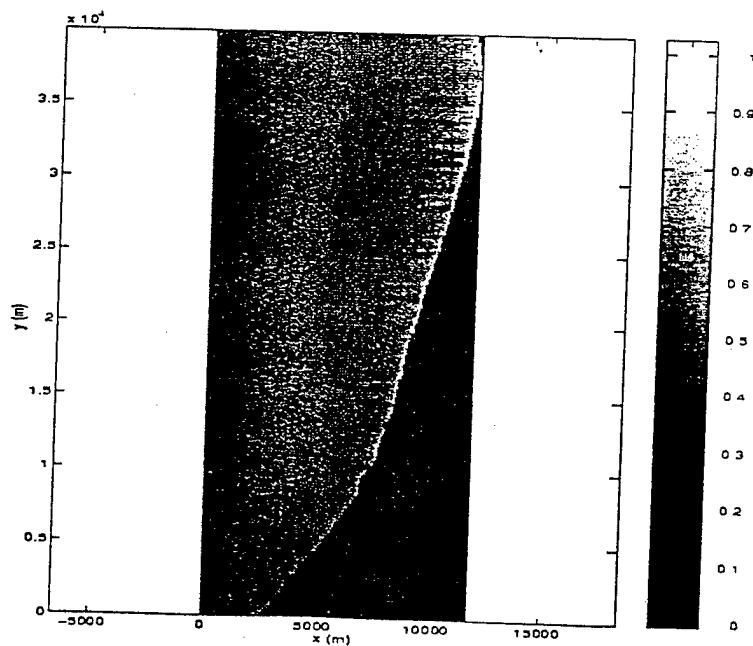


Figure 8: Partial Wave Height Field for August 11, 1997, 908PST. Model Forced with Portion of Buoy Spectrum ( $27.5^\circ$ - $72.5^\circ$  AZ and 0.04-0.13Hz). Heights are in Meters.

The REF/DIF1 model was run for the domain shown in Figure 9. Allard et al. (1998, this conference) used a  $2^\circ$  angular resolution for directions ranging from  $-70$  to  $+70$  degrees relative to the model grid  $x$  direction. No grid rotation was used to model higher incident angles. The frequency resolution for waves up to  $0.2\text{Hz}$  was  $0.01\text{Hz}$ .

Because the shelf is broad, with some bathymetric complexity in the nearshore, some sensitivity of the forecasting system to spectral discretization would be apparent. We analyze the discretization effects in the same manner as was done for the West Coast narrow shelf case. We first investigated the effect of angular discretization on the resulting wave height fields. A bandwidth of  $5.5^\circ$  was established around the mean direction. Six different levels of sub-bandwidth discretization were used:

- 1) One bin with  $5.5^\circ$  bandwidth.
- 2) Two bins of  $2.75^\circ$  bandwidth.
- 3) Four bins of  $1.375^\circ$  bandwidth.
- 4) 11 bins of  $0.5^\circ$  bandwidth.
- 5) 22 bins of  $0.25^\circ$  bandwidth.
- 6) 44 bins of  $0.125^\circ$  bandwidth.

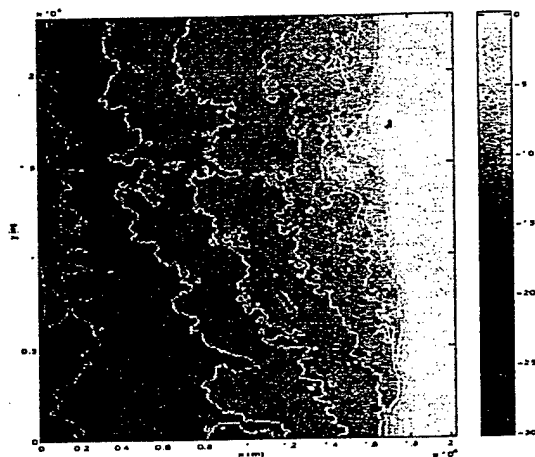


Figure 9: Domain of Study - Camp Lejune, NC. Depths Are In Meters.

This was done for several mean periods, and each frequency-direction bin was given a unit wave height. Figure 10 shows a result for a  $17\text{s}$  wave with a mean direction of  $-20^\circ$  to the  $x$ -axis of the grid. The bottom panel shows a single wave angle of  $-20^\circ$ . The middle panel shows the result of averaging four bins of  $1.375^\circ$  bandwidth and the top panel displays the result of averaging 44 bins of  $0.125^\circ$  bandwidth. Unlike the

West Coast case, there seems to be a distinct difference between the single component result and the averaged band results.

We also investigated the effect of averaging over several frequency bins within a single frequency band in order to represent the propagation of wave energy in that band. Seven sub-bandwidth levels of discretization were used:

- 1) One bin with  $0.06\text{Hz}$  bandwidth.
- 2) Two bins with  $0.03\text{Hz}$  bandwidth.
- 3) Six bins of  $0.01\text{Hz}$  bandwidth.
- 4) Ten bins of  $0.006\text{Hz}$  bandwidth.
- 5) 20 bins of  $0.003\text{Hz}$  bandwidth.
- 6) 40 bins of  $0.0015\text{Hz}$  bandwidth.
- 7) 50 bins of  $0.0012\text{Hz}$  bandwidth.

As before, this was done for several mean periods and a direction of  $-20^\circ$  from the  $x$  direction of the grid. All components were initialized with a unit wave height. Figure 11 shows a result for a wave with a mean period of  $12.5\text{s}$ . The lower panel shows the result for a single component at the mean period. The middle panel shows the result of six bins comprising a total bandwidth of  $0.06\text{Hz}$  about the mean frequency. The top panel shows the result of averaging over 50 bins within the  $0.06\text{Hz}$  bandwidth. There is some difference between the single component ~~run~~ and the averaged band results, again in contrast to the West Coast case.

It is instructive to investigate the variations of the individual bands comprising a bin prior to averaging, and compare their behaviors to that of the single component result as well as the averaged result. Figure 12 shows the waveheights and nearshore wave angles resulting from each of the individual 11 components making up a  $5.5^\circ$  band with a mean angle of  $-20^\circ$  to the grid. The nearshore point was located at  $x=13800\text{m}$ ,  $y=12900\text{m}$ , and the period  $T=17\text{s}$ . The water depth at this point was  $9.6\text{m}$ . The incident wave directions used at the offshore boundary are noted above each point. These are compared to the result from a single component with the mean offshore angle (solid black line), as well as the result of the average of all 11 components (dashed line). Not only is the scatter about the single component result significant, but there is a significant difference between this single component and the average of the 11 individual components comprising this band. As the directional resolution increases, both the amount of scatter and the value of the average vary less for increasing resolutions.

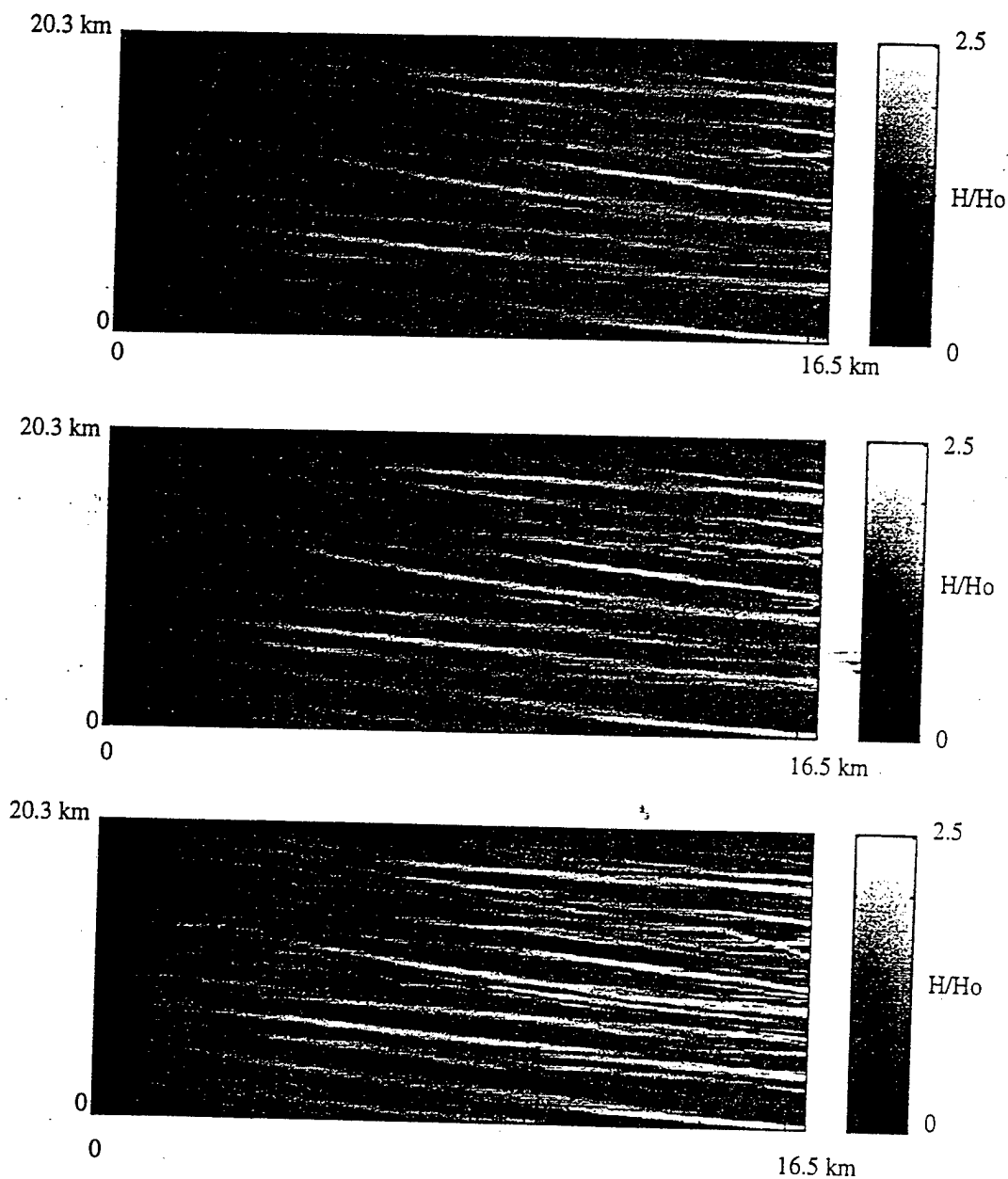


**Figure 10: Comparison of Directional Discretization Methods, Broad Shelf Case,  $T=17s$ , Mean Direction  $-20^\circ$  With Respect To Grid. Top:  $H/H_o$  Field from Average of 44 Components Within Band. Middle:  $H/H_o$  Field from Average of Four Components Within Band. Bottom:  $H/H_o$  Field from Single Wave Component at Mean Frequency and Direction. Note: Scale of Abscissa Distorted Relative To Ordinate.**

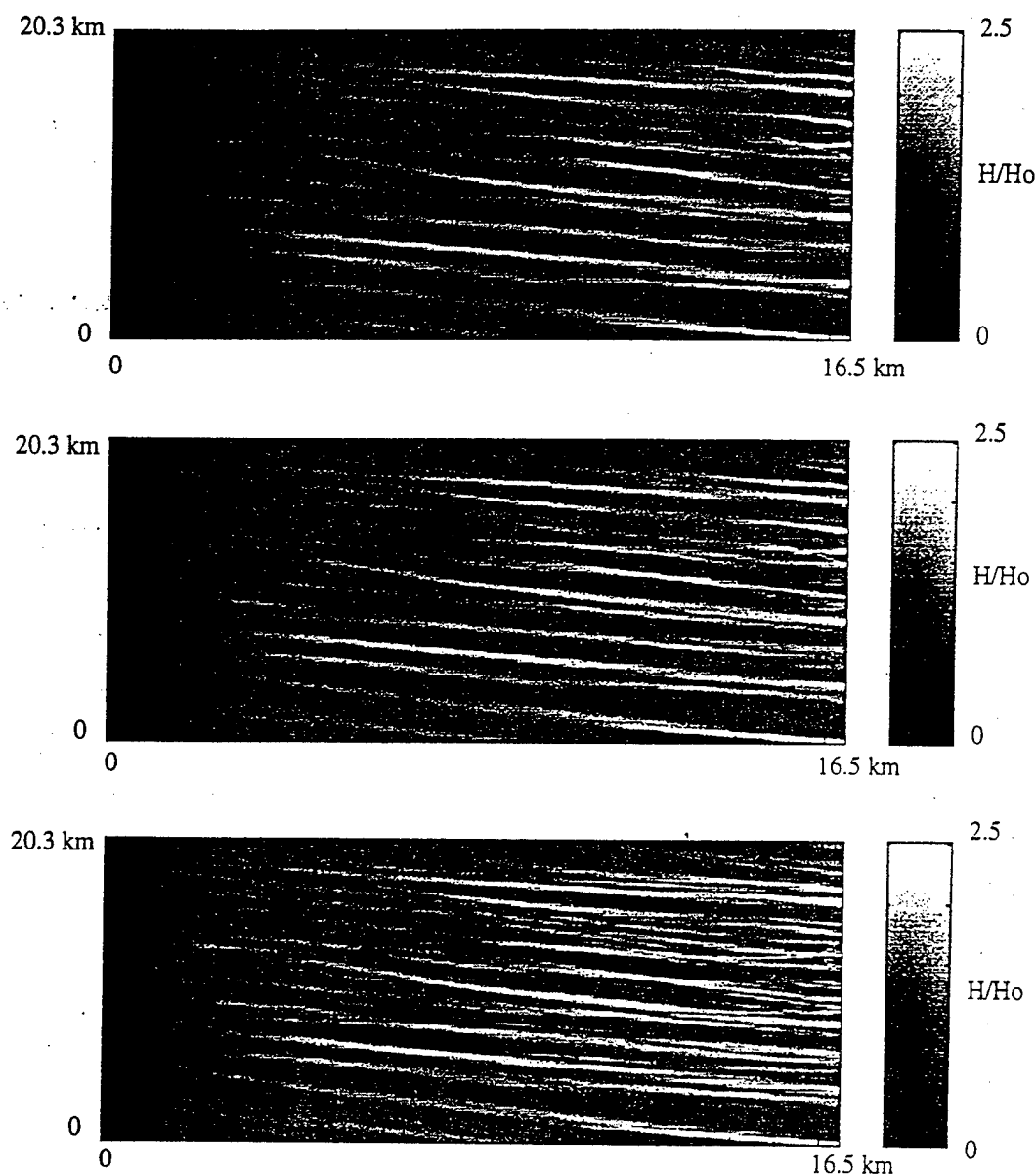


**Figure 11: Comparison of Frequency Discretization Methods, Broad Shelf Case,  $T=12.5s$ , Mean Direction  $-20^\circ$  With Respect To Grid. Top:  $H/H_o$  Field from Average of 50 Components Within Band. Middle:  $H/H_o$  Field from Average of Six Components Within Band. Bottom:  $H/H_o$  Field from Single Wave Component at Mean Frequency and Direction. Note: Scale of Abscissa Distorted Relative To Ordinate.**

In order to analyze the effect increasing the spectral resolution has on the wave height prediction, we investigated the convergence of the waveheight prediction to a particular waveheight field as the spectral resolution increases. Both frequency and directional resolution were analyzed. In the case of angular discretization, the highest directional resolution (44 bins, each of  $0.125^\circ$  bandwidth, comprising a  $5.5^\circ$  band about an incident angle of  $-20^\circ$ ) was taken to be

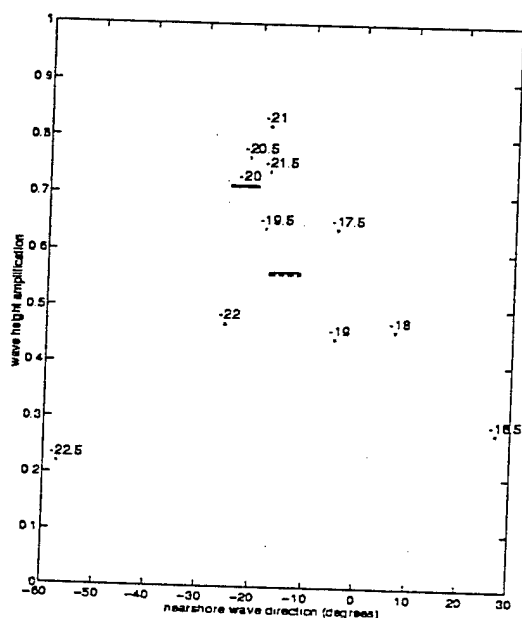


Figure 12: Predicted Nearshore  $H/H_o$  and Wave Angles for  $T=17s$ ,  $x=13800m$ ,  $y=12900m$ . Offshore Wave Angles are Noted Above Each Point. Black Dots: Results for 11 Individual Components Comprising a  $5.5^\circ$  Band. Solid Line: Result for Single Component at the Center Frequency and Direction. Dashed Line: Average of 11 Components.

the baseline for our comparisons. Differences between this baseline and the waveheights found using the other spectral resolutions were calculated and then averaged over the area of the grid seaward of the point of breaking. This yielded a "global mean error" for the particular discretization. Figure 13 shows the trend of the global mean error with decreasing directional bandwidth. The  $T=10s$  (top panel) and  $T=17s$  (lower panel) are shown in the figure. The convergence is almost exponential with bandwidth size. The  $17s$  wave seems to exhibit a slightly smaller overall error than the  $10s$  wave. It is apparent that the transformation characteristics of waves in the shallow water range do not vary as much with small variations in incident

angle as intermediate depth waves. The exponential behavior of the convergence curves also reveals the relative sensitivity of the results with variations in directional bandwidths for the larger bandwidth sizes.

A similar analysis was also performed for the frequency resolution. The highest frequency resolution used (50 bins with width of  $0.0012Hz$ , comprising a total frequency bandwidth of  $0.06Hz$ ) was used as the baseline in this case. Differences between the waveheight field from this baseline and those of the other frequency resolutions employed were calculated and averaged over the entire domain seaward of the point of breaking. Figure 14 shows the result of this analysis. The top panel displays the result for  $T=3.33s$ , the middle panel shows the result for  $T=7.14s$ , and the bottom panel shows the result for  $T=12.5s$ . Unlike the case of angular discretization, the convergence rate is linear rather than exponential. This indicates that the results would not be as quick to degrade relative to the baseline with degradation in frequency resolution as with degradation in angular resolution. Additionally, it also attests that the refraction/diffraction patterns for waves closely spaced in frequency are more similar than for waves closely spaced in direction. Additionally, also unlike the angular discretization case, the longer period wave has higher error for any particular frequency discretization than waves of lower period. This is sensible since a given frequency difference translates into a greater range of wavelengths for the lower frequencies. The above analyses for the broad shelf case indicates that the chosen frequency and direction discretizations used by Allard et al. (1998) are likely sufficient for the waveheight predictions.

It should be emphasized that the analyses outlined above were initialized with unit wave heights and performed in areas outside the surf zone. Thus the results are applicable to this bathymetry and the analyzed wave periods and directions regardless of initial wave height. However, extrapolation of these results to other domains should be done with care.

## 6. CONCLUSIONS

Phase-resolving numerical models offer an accurate description of monochromatic swell wave propagation over highly variable bathymetry. The simulation of irregular wave propagation using these models requires some care in how the spectra are discretized, since the smoothness of the resulting waveheight fields are often contingent on the fineness of the discretization.

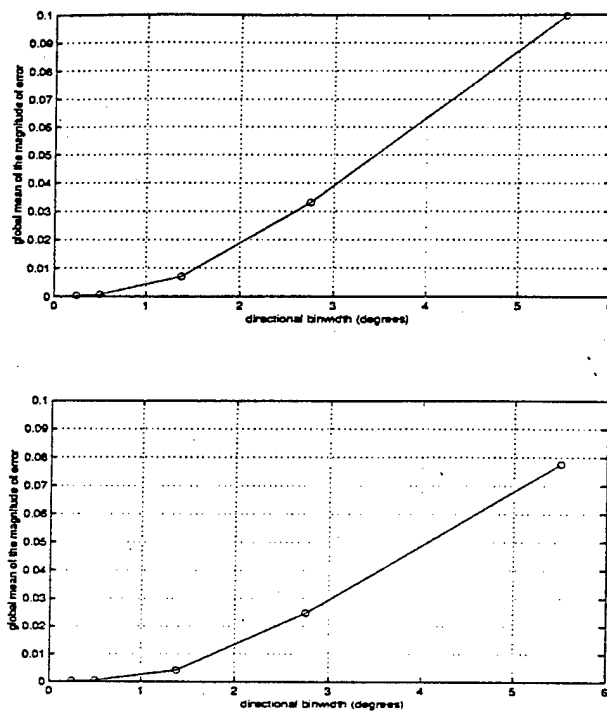


Figure 13: Rate of Convergence of Waveheight Results For Different Directional Binwidths to Baseline Waveheight Field. Top:  $T=10s$ . Bottom:  $T=17s$ .

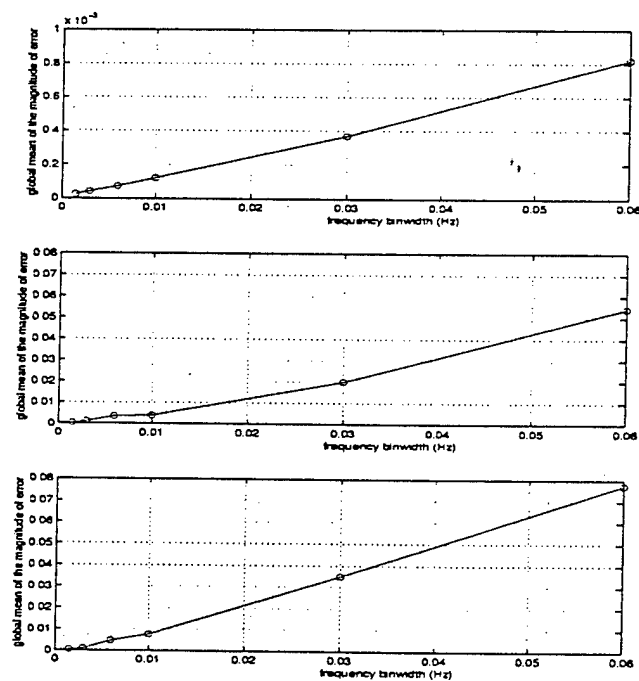


Figure 14: Rate of Convergence of Waveheight Results For Different Frequency Binwidths to Baseline Waveheight Field. Top: Mean Period=3.33s. Middle: Mean Period=7.14s. Bottom: Mean Period=12.5s.

We investigated two sites: Oceanside/Camp Pendleton, CA, and Camp Lejune, NC. A narrow shelf and relatively smooth bathymetry characterize the West Coast site, while the East Coast site has fairly complex bottom contours and distinct bottom features. We detailed the development of a forecasting system for the West Coast site, and also determined that the spectral discretization used in this system was sufficiently fine in frequency and direction. This was due to the fact that our grid was situated well leeward of the islands in the Southern California Bight, and thus did not have to account for the variations with frequency and incident direction in the refraction and diffraction patterns around them.

The East Coast Site did exhibit some sensitivity to the spectral discretization used, though it was determined that the frequency and direction bins used by Allard et al. (1998, this conference) appeared to be sufficiently fine to yield smooth waveheight fields. Exploring this further, we looked at the convergence of the waveheight field found by averaging over various numbers of subintervals in a frequency/direction band, to a set baseline. The convergence of the waveheight field to the baseline was found to be nearly exponential when varying the directional discretization, and nearly linear when varying the frequency discretization.

The general conclusion of this study is that spectral discretization can play a potentially important role in the accuracy and smoothness of a prediction of waveheight (and ensuing processes), and its importance seems to be in direct proportion to the complexity of the underlying bathymetry. The study also emphasizes the need to model irregular wave fields in multi-component (rather than pseudo-monochromatic) fashion, since wave response characteristics may vary greatly with small variations in frequency and/or incident direction.

## 7. ACKNOWLEDGMENTS

Both JMK and WER were supported by the Office of Naval Research through the Naval Research Laboratory, Stennis Space Center, MS, under the 6.2 "Coastal Simulation" NRL Core project. YLH was supported by Space and Naval Warfare Systems Command. BOR was supported by the State of California Department of Boating and Waterways. Discussions with Dr. Robert Jensen (Coastal and Hydraulics Laboratory, U.S. Army Waterways Experiment Station, Vicksburg, MS) and Mr. Paul Wittmann (Fleet Numerical Meteorological and Oceanographic Center, Monterey, CA) concerning the WAM model were very informative. This paper, NRL

contribution PP/7322-97-0042, is approved for public release; distribution unlimited.

## 8. REFERENCES

- Allard, R.A., Y.L. Hsu, J.M. Smith, M.D. Earle, T. Mettlach, and K. Miles, 1998: Use of coupled numerical wave models to simulate the littoral environment from deep water to the beach. Proceedings of the 5<sup>th</sup> International Workshop on Wave Hindcasting and Forecasting, Melbourne, FL.
- Berkhoff, J.C.W., 1972: Computation of combined refraction-diffraction. Proceedings of the 13<sup>th</sup> International Conference on Coastal Engineering, 471-490, Vancouver, BC.
- Booij, N, L.H. Holthuijsen, and R.C. Ris, 1996: The SWAN wave model for shallow water. Proceedings of the 25<sup>th</sup> International Conference on Coastal Engineering, 668-676, Orlando, FL.
- Dally, W.R., R.G. Dean, and R.A. Dalrymple, 1985: Wave height transformation across beaches of arbitrary profile, *J. Geophys. Res.*, 90, 2035-2043.
- Ebersole, B.A., M.A. Cialone, and M.D. Prater, 1986: Regional coastal processes numerical modeling system: RCPWAVE - a linear wave propagation model for engineering use. Technical report CERC-86-4, Coastal Engineering Research Center, U.S. Army Waterways Experiment Station, Vicksburg, MS, 71p.
- Kirby, J.T., 1986: Higher order approximations in the parabolic equation method for water waves, *J. Geophys. Res.*, 91, 933-952.
- Kirby, J.T., and R.A. Dalrymple, 1994: Combined refraction/diffraction model REF/DIF1, version 2.5, documentation and user's manual. CACR report 94-22, Center for Applied Coastal Research, University of Delaware, Newark, DE, 171p.
- Komen, G.J., L. Cavaleri, M.A. Donelan, K. Hasselmann, S. Hasselmann, and P.A.E.M. Janssen, 1994: Dynamics and modeling of ocean waves, Cambridge University Press, Cambridge, U.K., 532p.
- O'Reilly, W.C., and Guza, R.T. 1993: A comparison of two spectral wave models in the Southern California Bight, *Coast. Eng.*, 19, 263-282.



Radder, A.C., 1979: On the parabolic equation method for water wave propagation, *J. Fluid Mech.*, 95, 159-176.

Resio, D.T., 1988: A steady state model for coastal applications, Proceedings of the 21<sup>st</sup> International Conference on Coastal Engineering, 929-940, Malaga, Spain.

Wittmann, P.A., and P.D. Farrar, 1997: Global, regional and coastal wave prediction. *MTS Journal*, 31, 76-82.